Invited Articles

Bubble dynamics in complex fluids

Valeria Garbin *

Department of Chemical Engineering, Delft University of Technology, Delft, The Netherlands

(Received 29 July 2025; accepted 5 November 2025; published 7 January 2026)

The field of bubble dynamics and cavitation, motivated initially by applications in underwater acoustics and later in biomedical ultrasound, continues to evolve. This article describes the recent focus and ongoing developments in understanding and utilizing bubble dynamics in complex fluids. An introductory overview is given of the phenomena of spherical bubble dynamics in complex fluids. The emerging interest in using bubble dynamics to probe high-frequency viscoelastic properties of complex fluids is then highlighted. This interest is motivated by the fact that timescales as short as 10^{-6} s can be probed, comparable to the relaxation timescales for complex fluids containing suspended particles or macromolecules. The focus of the article then shifts to specific examples from my research group. First, I present our work on linear rheology of soft solids using ultrasound-driven bubbles. I then discuss how the deformation and flow fields generated by acoustically driven bubbles can modify the microstructure and properties of complex fluids, bearing potential for bubble removal from yield-stress fluids. Finally, I describe our observations of self-assembly of locally ordered microstructures in complex fluids driven by bubble dynamics. In closing, I discuss the growing synergy between the communities of cavitation and rheology, which will be instrumental to address new challenges in the characterization and manipulation of complex fluids.

DOI: 10.1103/hj5m-fcvt

I. INTRODUCTION

The presence of bubbles in complex fluids and soft matter is widespread in natural and artificial systems that span multiple decades in length scales (Fig. 1). At the kilometer scale of volcanoes, bubbles grow by exsolution during decompression of ascending magma [1], a complex fluid with nontrivial, time-dependent rheology. At the centimeter scale of leaves, tensile stresses due to evaporation can cause bubble nucleation in trees [2]. For biomedical applications of ultrasound, micron-sized bubbles are manufactured and used for both ultrasound medical imaging [3] and drug delivery [4]. Cavitation at the scale of single cells is suspected to play a role in neurostimulation by ultrasound, but the mechanism is yet to be fully elucidated [5]. Finally, bubble nucleation and cavitation in complex fluids is relevant in many industrial processes, from food processing to manufacturing of materials. The classical example of the manufacture of polymer foams motivated one of the earliest studies on bubble motion in viscoelastic liquids [6]. More recently, in the ultrasonic processing of nanomaterials, the length-dependent flow behavior of carbon nanotubes around cavitation bubbles was found to explain the resulting size distributions [7]. In these examples,

*Contact author: v.garbin@tudelft.nl

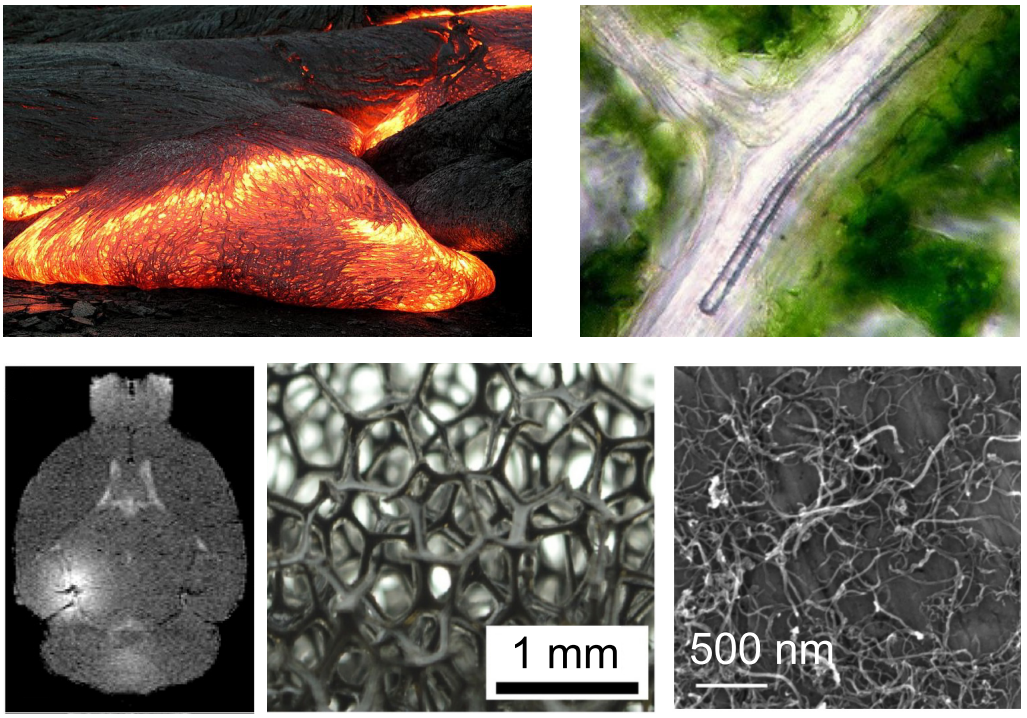

FIG. 1. Bubbles in complex fluids. Top: From the kilometer scale of volcanoes (left; USGS, public domain), to the centimeter scale of plant leaves (right; adapted from [9] with permission from Springer). Bottom: Biomedical application of microbubbles in blood brain barrier opening (left; reproduced from [10]), industrial applications in the manufacture of polymer foams (middle; adapted from [11].), and ultrasonic processing of carbon nanotubes (right adapted with permission from [12]. Copyright 2009 American Chemical Society).

it is crucial to understand and quantify the effect of viscoelastic properties of the surrounding complex fluid on bubble dynamics. Conversely, in many of the examples, bubble dynamics are found to affect—and can ultimately be used to manipulate—the surrounding complex fluid. The mathematical description of the effect of viscoelastic properties of the surrounding medium on bubble dynamics has been reviewed recently [8]. This article first provides a high-level overview of ongoing developments in the field, then focuses on recent advances made by our research group, and, finally, highlights questions that remain open for future research.

Before addressing the effect of a viscoelastic medium on bubble dynamics, one must first recognize that bubble dynamics are highly nonlinear even in simple fluids, as shown in the classical theory of bubble dynamics by Prosperetti and Plesset [13]. Despite this complexity, our understanding of bubble dynamics in simple fluids is now sufficiently advanced that it can be built upon. From the seminal work of Lord Rayleigh on the collapse of a cavity [14] to the explanation of single bubble sonoluminescence [15], a widely accepted theoretical framework exists for describing bubble collapse under idealized conditions. With the Rayleigh-Plesset equation, we can describe spherical bubble collapse as well as spherical bubble oscillations driven by pressure fluctuations [13]. For small-amplitude oscillations, we can describe bubbles as harmonic oscillators and use linear theory to analyze their resonance behavior [16]. To extend the analysis to complex fluids, one can generalize the Rayleigh-Plesset equation [17], which is derived for a Newtonian liquid, to account for the material properties of the complex fluid through the deviatoric stress tensor, $\boldsymbol{\tau}$. Indeed, rather than by a constant, Newtonian viscosity, a complex fluid can exhibit non-Newtonian behavior, as well as elastic, solidlike behavior [18]. Furthermore, the viscous and elastic properties may depend on time, on the strain amplitude or strain rate, and on the history of deformation.

Research in the field of rheology has led to the development of constitutive models for many of these behaviors [19], some of which have been successfully combined with the modified Rayleigh-Plesset equation, as briefly explained in the following.

Consider a spherical bubble in a quiescent, incompressible, complex fluid. We limit the analysis to a homogeneous, isotropic medium, keeping in mind that complex fluids can, in some situations, also exhibit inhomogeneous or anisotropic properties [18]. Assume that the bubble has a fixed position with its center at the origin of a spherical coordinate system (r, θ, ϕ). The equation governing the time evolution of the bubble radius R is then [17]

$$\rho\left(R\ddot{R} + \frac{3}{2}\dot{R}^2\right) = p(R) - p_\infty + \int_R^\infty (\nabla \cdot \boldsymbol{\tau})_r dr, \tag{1}$$

where ρ is the density of the medium, the dot denotes the derivative with respect to time, p_∞ is the pressure in the medium far from the bubble, and $p(R)$ is the pressure in the medium at the bubble interface. The term $(\nabla \cdot \boldsymbol{\tau})_r$ is the radial component of $\nabla \cdot \boldsymbol{\tau}$, the divergence of the deviatoric stress tensor. Early attempts at modeling bubble dynamics in viscoelastic media were focused on linear viscoelastic effects, valid for small-amplitude deformation of the material: the linear Maxwell model for a viscoleastic liquid [20] and the Kelvin-Voigt model for a viscoelastic solid [21]. To describe an intermediate behavior between fluid and solid, the two constitutive models can be combined into the the Standard Linear Solid model, which has been combined with the Keller-Miksis equation for bubble dynamics [22]. For large deformations, a nonlinear constitutive model can be combined with the equation governing bubble dynamics, which in this case should also account for compressibility effects. Several nonlinear versions of the Maxwell model have been considered for viscoelastic liquids [23–26] while for viscoleastic solids, the effect of nonlinear elasticity has also been analyzed [27]. A recently proposed approach is to formulate the medium rheology through a relaxation function, thereby generalizing the Rayleigh-Plesset equation to materials with arbitrary rheology [28].

An equation governing spherical bubble dynamics—the Rayleigh-Plesset equation or a modification accounting for compressibility effects—combined with a constitutive model for the medium rheology can be seen as a tool to study complex fluids, with two important advantages, which are discussed in more detail in [29]. First, the flow field around a spherically deforming bubble is well defined. The flow is purely elongational, and a range of strains is probed in the same experiment, as shown in Fig. 2(a) where the magnitude of the stretch $\ell(t)$ of each fluid element is color coded. Second, there are three distinct phenomena resulting in spherical bubble dynamics which cover a broad range of timescales, while being sensitive to the properties of the surrounding medium. Of the three phenomena considered, bubble collapse and bubble oscillations are described by Eq. (1), while bubble dissolution is described by a modified Epstein-Plesset equation [30,31]. The effect of the elastic modulus G is exemplified in Figs. 2(b)–2(d) by computing the temporal evolution of the bubble radius, assuming simple constitutive models for the surrounding (visco)elastic medium, as explained below. Bubble collapse, shown in Fig. 2(b), can probe timescales as short as 10^{-7} s, which are difficult to access in a controlled manner with other experimental methods. Spherical bubble oscillations [Fig. 2(c)], for instance driven by an acoustic field, impose an oscillatory elongational deformation at controlled frequency and they probe timescales of the order of 10^{-6}–10^{-3} s, also difficult to access otherwise. Both Figs. 2(b) and 2(c) are obtained by solving Eq. (1) for a viscoelastic medium with neo-Hookean elasticity G and Newtonian viscosity η. Finally, if we consider a different mechanism of spherical bubble dynamics, which is dissolution or growth by mass transfer (depending on the gas saturation in the medium, ζ), then we again have the same deformation field and slow timescales of deformation of the order of 10^3 s. Figure 2(d), obtained by solving the Epstein-Plesset equation [30] modified for a neo-Hookean, purely elastic surrounding medium of shear modulus G [31], shows that elasticity affects bubble dissolution and can arrest it. Together, these three distinct phenomena cover 10 decades in deformation frequency, all with a well-defined, elongational deformation field of the fluid. For these reasons, there has been significant work in the bubble dynamics community to use bubble dynamics in complex fluids and soft solids

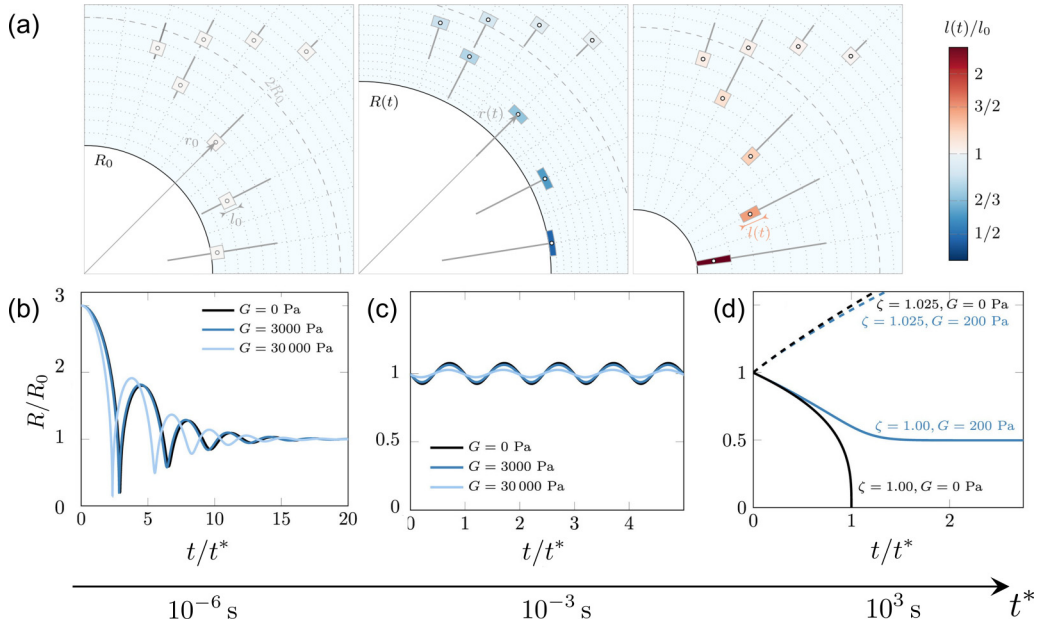

FIG. 2. Spherical bubble dynamics spanning 10 decades in timescales. (a) Elongational deformation field around a spherically deforming bubble, with R_0 the initial radius, $R(t)$ the time-dependent radius, and ℓ the stretch of a fluid element. Effect of medium elasticity G on three distinct phenomena: (b) bubble collapse, (c) bubble oscillations, and (d) bubble dissolution or growth by mass transfer, where ζ is the gas saturation in the surrounding medium. Adapted from [29] with permission from Elsevier.

to either understand the effect of the medium on bubble dynamics or to extract properties of the medium, as discussed in [8].

In this article, I will mainly describe recent experimental findings from my research group based on ultrasound-driven bubble oscillations as a platform for controlled deformation of complex fluids. The technical aspects of the experiments are not reported in extensive detail here, as they can be found in the respective publications. The emphasis is on the unexpected observations that led us to new research directions. The article also provides the context of the current state of the art, with reference to significant contributions by other research groups. Section II describes the application of bubble dynamics to probe the rheology of complex fluids. In Sec. III, yield stress is introduced and yielding by bubble oscillations is discussed. In Sec. IV, the heterogeneous microstructure of a complex fluid is taken into account and the evolution of the microstructure caused by bubble dynamics is examined. Finally, in Sec. V, I will discuss ongoing developments in this growing field at the crossroads of fluid dynamics, rheology, and soft matter physics.

II. BUBBLE DYNAMICS TO PROBE HIGH-FREQUENCY RHEOLOGY

In the last decade, the three bubble dynamics phenomena introduced in Sec. I have been proven by different research groups to be sensitive to the rheology of the surrounding medium in controlled experiments (Fig. 3), thus laying the foundations for the application of bubble dynamics for the rheological characterization of complex fluids. A bubble can be either laser or spark generated, typically for bubble collapse experiments, or it can be injected in the medium. The latter approach proves particularly challenging for certain complex fluids, as will be discussed later in Sec. III. Once a bubble is present in the medium, the experimental data for the temporal evolution of the radius, $R(t)$, can be fitted to the predictions of a model combining the governing equation for bubble

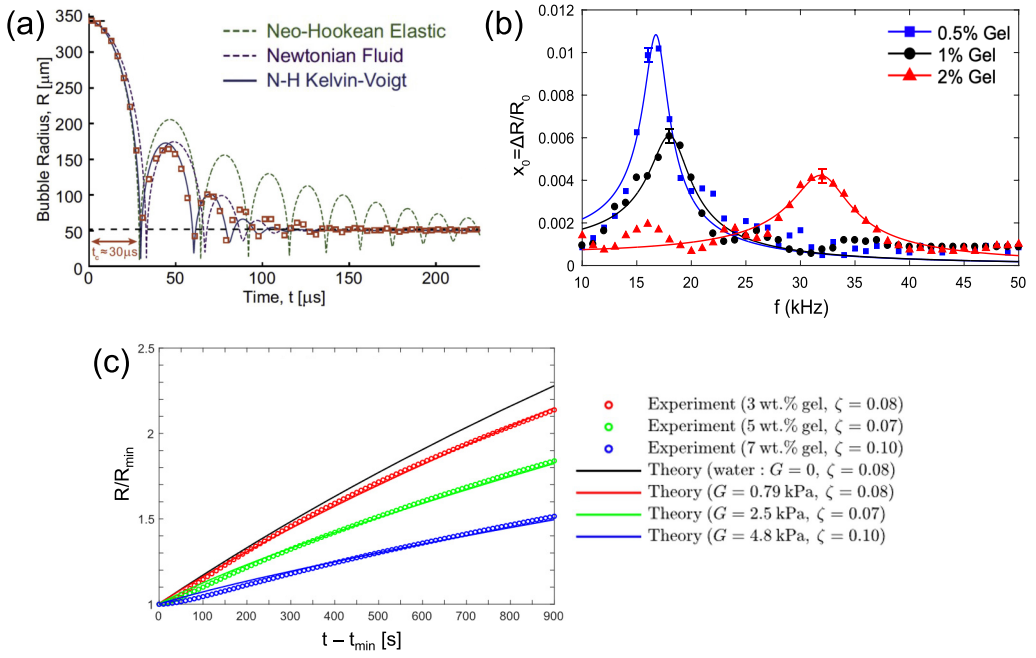

FIG. 3. Measuring medium rheology from bubble dynamics. (a) Bubble collapse at 10^{-5} s timescale, reproduced from [32] with permission from Elsevier. Experimental data of collapse dynamics of a laser-generated bubble in a polyacrylamide gel are compared with the best fits for different constitutive models of the medium. A neo-Hookean Kelvin-Voigt viscoelastic solid model (blue solid line) gives the best fit and provides estimates of the elastic modulus G and viscosity η. (b) Resonance curves for linear bubble oscillations at 10^{-3} s timescale, reproduced from [33]. Experimental data for the normalized oscillation amplitude, x_0, are fit to resonance curves from linear theory with a Kelvin-Voigt constitutive model. For agarose hydrogels of increasing concentration, the resonance frequency increases due to the increased elasticity G [see Eq. (2)], while the increased viscous damping broadens the resonance peak. (c) Bubble growth by mass transfer at 10^3 s timescale, reproduced from [34] with permission from the American Institute of Physics. Laser-generated bubbles in air-saturated gelatin grow by mass transfer. The growth dynamics can be fitted to estimate the saturation coefficient ζ and the elastic modulus G of the medium.

dynamics with an appropriate constitutive model for the complex fluid, enabling extraction of its rheological properties [29].

The method based on bubble collapse, termed "inertial microcavitation rheometry," was first introduced by Estrada *et al.* [32]. Figure 3(a) shows the experimental results and model predictions from [32] for a laser-generated bubble in a polyacrylamide gel. Testing of different constitutive models showed that a neo-Hookean Kelvin-Voigt constitutive model—with both elastic and viscous components—accurately fits the bubble collapse dynamics and enables estimation of the elastic modulus G and viscosity η. These methods has been further developed by generating the bubbles acoustically using focused ultrasound [35], by applying data assimilation techniques [36], and by introducing reduced-order models [37].

Our group has focused on linear bubble oscillations of controlled amplitude and frequency driven by ultrasound. Figure 3(b) shows an example for agarose hydrogels [33]. We injected a spherical bubble in the hydrogel before complete gelation. Agarose hydrogel is optically transparent and the rheological properties can be easily tuned. We used a microbubble spectroscopy approach [38] to construct the resonance curves of bubbles in gels with different concentration. The bubble was driven with ultrasound at 10–50 kHz and with sufficiently small acoustic pressure amplitude that

the bubble dynamics remained linear. We see in Fig. 3(b) that the increase in concentration causes increasingly more damping and a shift of the resonance frequency. Because the bubble oscillations are linear and we also worked in the regime of linear deformation of the material [33], following [21] we can then use the linear Kelvin-Voigt constitutive model for the stress tensor in Eq. (1) and apply linear theory to obtain an expression for the resonance frequency ω_0 that allows us to quantify the elastic modulus G,

$$\omega_0^2 = \frac{1}{\rho R_0^2}\left[3\kappa p_0 + \frac{2(3\kappa - 1)\gamma}{R_0} + 4G\right], \tag{2}$$

where R_0 is the equilibrium bubble radius, κ is the polytropic exponent quantifying deviations from ideal gas behavior, p_0 is the ambient pressure, and γ is the interfacial tension of the gas-liquid interface. The extracted values of G were higher for higher agarose concentration, as expected. We also compared the values with the measurements from a standard rotational rheometer operating at a frequency of 10 Hz. We found that the material is stiffer for higher deformation frequency, as expected for agarose gels. This finding also indicates that care must be taken when selecting a linear constitutive model, which assumes constant viscoelastic parameters (i.e., independent of frequency).

While the third mechanism, bubble dissolution or growth, does not probe high-frequency properties, it is also of interest as it probes the other extreme of the range, with timescales of the order of 10^3 s, as shown in Fig. 2. Experimental results from Ando and Shirota [34] are shown in Fig. 3(c), demonstrating the effect of an elastic medium (gelatin) on delaying bubble growth by diffusion in a supersaturated medium. Fitting the bubble growth dynamics to a model including a neo-Hookean elastic surrounding medium [31] provides estimates of both the saturation coefficient ζ and the elastic modulus G.

The growing interest in measuring high-frequency or high-strain-rate properties of soft materials is motivated by several applications in biomedical ultrasound [4,39], where deformations are driven at the fast timescales of ultrasound itself; but fast flow conditions are also typical in processing flows such as ink-jet printing [40]. From a more fundamental standpoint, high-frequency properties are associated with the fast relaxation timescales of materials, which gives insights into the microstructure [18]. At the other extreme of the range, low frequencies and long timescales are relevant for stability and shelf life of many consumer products based on complex fluids with dispersed bubbles.

III. NONLINEAR EFFECTS: YIELDING BY BUBBLE OSCILLATIONS?

Nonlinear effects in the complex fluid's response to deformation complicate matters significantly. An intriguing nonlinear effect is the change in material properties upon deformation known as *yield stress*: the material behaves as a solid below a threshold in stress, and as a liquid above it. Complex fluids that exhibit such property are typically systems in which drops, bubbles, or particles are jammed together, and a certain stress is required to unjam the configuration; or systems with attractive interactions, where stress is needed to break interparticle bonds [41].

Bubbles can be trapped if the stress due to buoyancy is below the yield stress τ_Y, as expressed by the Bingham number $\mathrm{Bn} = \frac{\tau_Y}{\Delta\rho g R_0}$, where $\Delta\rho$ is the density difference, g the acceleration due to gravity, and R_0 is the equilibrium bubble radius. A yield stress as small as 10 Pa is sufficient to trap bubbles of 1 cm. If the bubble is sufficiently large and the buoyancy force applies a sufficient stress to overcome the yield stress, a region of the fluid "switches" from solid to liquid and the bubble can rise [42]. Trapping, motion, and growth of bubbles in yield-stress fluids [43–45] is relevant because control of bubbles, which can be desirable or not, is key in many situations involving these complex fluids, from formulated products, to construction materials, to gas transport in soil.

Our group set out to investigate whether bubble oscillations driven by ultrasound could help release bubbles from yield-stress fluids, not by virtue of an increased buoyancy force, but by using the oscillatory deformation of the medium to fluidize it locally [46,47]. We know that the deformation is high frequency, but are the strain and the resulting stress sufficiently large? And can

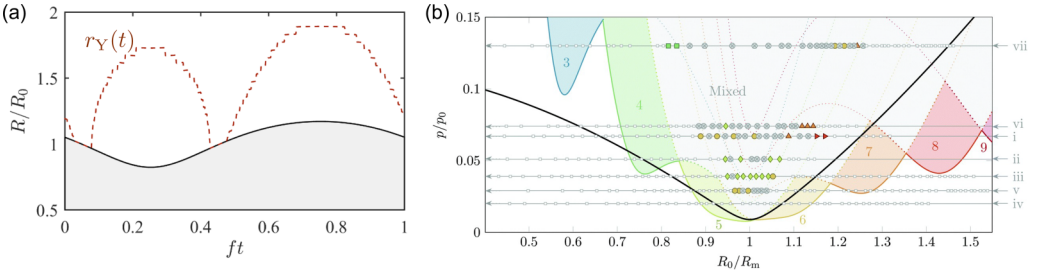

FIG. 4. Acoustic bubble dynamics in a yield-stress fluid. (a) Theoretical prediction from a model combining the Rayleigh-Plesset equation with a constitutive model for a visco-elasto-plastic medium. The oscillation frequency of the radius of the yielded region, r_Y, is twice the oscillation frequency of the bubble radius R. Reproduced from [46]. (b) Regime map for shape oscillations of bubbles in Carbopol as a function of the applied acoustic pressure p/p_0 and the initial radius of the bubbles, R_0/R_m, for a fixed driving frequency $f = 22.5$ kHz. The colored areas are theoretical predictions for the occurrence of modes $k = 3$–9, based on [51]. The symbols represent experimental results: white squares for stable spherical oscillations; gray, crossed circles for mixed modes; filled symbols for clear shape oscillations of mode k (with same color coding for k as the colored areas). The black solid line is the theoretical threshold for medium yielding. Reproduced from [47].

the bubble rise in the yielded region? Seminal theoretical work by Karapetsas *et al.* suggests that acoustic excitation can enhance the mobility of a gas bubble in a viscoplastic fluid [48], which was described using the Bingham constitutive model.

We first combined the modified Rayleigh-Plesset equation (1) with a constitutive model for the yield-stress fluid that takes into account both the elastic and viscoplastic deformations of the material, the elasto-viscoplastic model of Saramito [49]. We solved the model for Carbopol, of which we know the yield stress from shear rheological measurements. To determine if the fluid at a certain location is yielded, the classical von Mises criterion can be used, consistent with experimental measurements of the apparent elongational yield stress which were in agreement with the von Mises plasticity criterion [50]. The resulting model [46] predicts the bubble radius and tracks the evolution of the fluidized region around the bubble. Figure 4(a) shows the time evolution of the normalized bubble radius, R/R_0, and of the radius of the yielded region, r_Y/R_0, as a function of dimensionless time ft, where f is the oscillation frequency. The shaded area represents the region with radial coordinates $r < R_0$, where r_Y is not defined. The qualitative dynamics of r_Y are periodic, with twice the frequency of the bubble oscillations. That is, the yielded region reaches a maximum both during the half period of bubble expansion and during the half period of bubble compression, owing to the deformation of the fluid elements—uniaxial extension in the radial direction during bubble compression, and biaxial extension in the azimuthal and polar directions during bubble expansion [19]. The model also predicts the critical pressure for medium yielding, which can be tested in experiments.

To test the theoretical prediction of medium yielding by bubble oscillations, in our experiments we drove oscillations of a bubble in Carbopol, with the intention to indirectly detect medium yielding by observing bubble rise and taking care to not apply any acoustic radiation forces which would cause spurious bubble motion [47]. For acoustic pressures of sufficiently small amplitude to keep the bubble oscillations spherical, we detected no bubble rise. For higher-pressure amplitudes, shape instabilities occurred, accompanied by erratic motion of the bubbles, which does point to medium yielding despite not being effective for bubble removal. Linear stability predictions for shape oscillations of mode number k in Kelvin-Voigt soft solids [51] define regions in the (R_0, p) plane [see Fig. 4(b)] in which bubble oscillations either remain spherical or exhibit a single shape mode k, or mixed shape modes, for a fixed driving frequency f. In Fig. 4(b), the modes observed in experiments as a function of R_0 and p are shown for seven bubbles (labeled i–vii). Multiple acquisitions have been conducted on each bubble while it slowly dissolved, to explore

a range of values of R_0 with the frequency f and the pressure p kept constant. The threshold in pressure for shape oscillations reaches a single local minimum close to $R_0 = R_\mathrm{m}$, where R_m is the resonant radius based on the Minnaert frequency, $f_\mathrm{m} = \frac{1}{2\pi R_0}\sqrt{\frac{3\kappa p_0}{\rho}}$. The shape number k in our experiments increases with R_0, in qualitative agreement with the model predictions [51]. However, a more quantitative comparison with the model predictions is unsatisfactory. For instance, several experiments show stable spherical oscillations where the model predicts shape oscillations. A possible reason for the dynamic heterogeneity observed in the occurrence of shape instabilities may be related to bubble injection. Injecting bubbles in Carbopol without causing memory effects is notoriously difficult [52]. An additional limitation of the experimental approach is that multiple experiments are performed on the same bubble as it slowly dissolves, which may also introduce memory effects in the yield-stress material.

While the lack of bubble removal may be due to a combination of many factors (bubble size, viscosity, and elasticity of the yielded region; incorrect assumption on the value of the yield-stress under high-frequency elongational deformation), it is very difficult to interpret our observations because it is simply not possible to detect if Carbopol is yielded. A yield-stress fluid in which the microstructure can be visualized and characterized would greatly enhance our understanding of the effect of bubble dynamics on the material. This is indeed the subject of the next section.

IV. BUBBLE OSCILLATIONS IN YIELD-STRESS FLUID: EVOLUTION OF THE MICROSTRUCTURE

In an attempt to visualize and quantify the effect of bubble dynamics on a yield-stress fluid, we selected a material for which the microstructure can be observed by optical microscopy: a colloidal gel. The selected gel is made of colloidal particles of 400 nm in radius, with tuneable attractive interactions (10–20 $k_\mathrm{B}T$) via a polymer depletant, and a volume fraction of particles around 40%. This is a well-characterized model system that has been extensively used in studies of colloidal gels under shear flow [53]. To perform confocal microscopy in order to reconstruct the three-dimensional (3D) microstructure of the material, we adopted a Hele-Shaw geometry, where the bubble was flattened into a pancake to accommodate the limited depth of focus of a confocal microscope [54]. For such geometry of bubble confinement, the limited research available shows that the typical secondary flow around oscillating bubbles in confinement, known as *bubble microstreaming* [55–57], is also observed for bubbles flattened between two solid boundaries [58].

A striking change in the microstructure can be observed after applying 500–1000 cycles of ultrasound-driven bubble oscillations at 15 kHz, whereby the microstructure of the colloidal gel becomes locally ordered. This effect can be quantified by calculating the distribution of bond orientations, $\mathcal{P}(\phi^{ij})$, where the bond orientation ϕ^{ij} between reference particle i and a neighboring particle j is defined with respect to the line of centers between the bubble and the reference particle. $\mathcal{P}(\phi^{ij})$ is computed for each of the color-coded annular sectors shown in Figs. 5(a) and 5(b), of width $0.3R_0$ starting from R_0 to $2.5R_0$, with R_0 the equilibrium bubble radius. Before ultrasound-driven bubble oscillations, $\mathcal{P}(\phi^{ij})$ is almost flat, indicating no order [Fig. 5(c)]. After oscillations, two clear peaks emerge, at $\phi^{ij} = \pm\frac{\pi}{4}$, as shown in Figs. 5(d) and 5(g). The magnitude of the peaks decreases with distance from the bubble. The change in orientational order is also visible with the naked eye by comparing the micrographs in Fig. 5(e) before and Fig. 5(f) after bubble dynamics. In the region up to one bubble radius away from the bubble interface, the particles can be seen to exhibit orientational order along two principal directions, $\phi^{ij} = \pm\frac{\pi}{4}$, as shown schematically in Fig. 5(g). A microstructure with such peculiar orientational order has no counterpart in simple shear or oscillatory shear.

Several mechanisms simultaneously present in this system can be responsible for this rearrangement. The oscillatory flow at the frequency of ultrasound is sufficiently strong to break the interparticle bonds; this competition can be approximately captured by the Péclet number comparing the

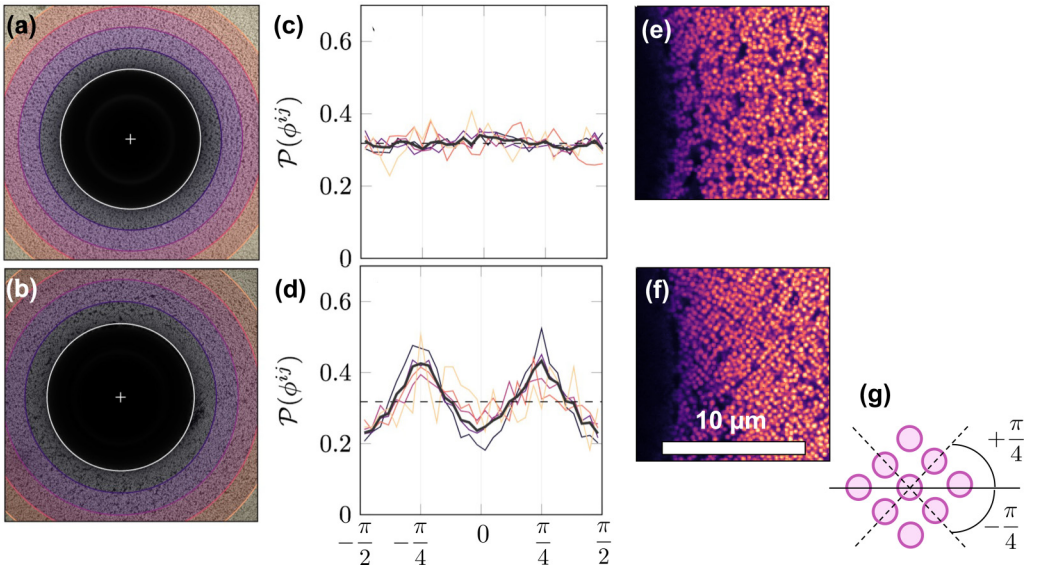

FIG. 5. Local order in a colloidal gel caused by ultrasound-driven bubble dynamics. The situation (a),(c),(e) before and (b),(d),(f),(g) after ultrasound-driven bubble dynamics. (a),(b) The domain around the bubble is segmented into bins to calculate the orientational order parameter $\mathcal{P}(\phi^{ij})$ as a function of distance from the bubble. (c),(d) The microstructure is characterized by an order parameter $\mathcal{P}(\phi^{ij})$ that measures orientational order with the respect to the line of centers between the bubble and a reference particle. No orientational order is visible in (c) before bubble dynamics, while two clear peaks emerge in (d) after bubble dynamics. Micrographs in (e) before and (f) after bubble dynamics with visible change in orientational order. The schematic in (g) shows the definitions of the directions $\phi^{ij} = \pm\frac{\pi}{4}$. Adapted from [54].

rate of the convective flow due to bubble oscillations to the rate of diffusion of colloids of radius a,

$$\mathrm{Pe}^{\mathrm{osc}} \approx \left(\omega \frac{\Delta R}{R_0}\right)\left(\frac{\eta a^3}{k_\mathrm{B}T}\right) \sim 10^3, \tag{3}$$

with ω the angular frequency of oscillations, ΔR the amplitude of oscillations, η the shear viscosity, and $k_\mathrm{B}T$ the thermal energy. The microstreaming flow around pancake bubbles [58] is weak and short ranged. In our experiments, its velocity is estimated at 1 µm s^{-1}; with such small velocity, the microstreaming flow cannot break interparticle bonds but could affect the microstructure. Finally, geometric frustration of a close-packed arrangement of spheres due to the circular domain can be ruled out since particle-based simulations without hydrodynamic effects show accumulation of particles near the bubble but do not show the characteristic $\phi^{ij} = \pm\frac{\pi}{4}$ order [59]. Further work is needed to fully elucidate the mechanism.

Even with an—as yet—incomplete understanding of the mechanism, it can already be exploited in applications. There is a lot of interest in structuring colloidal gels for applications in manufacturing of materials based on colloidal gels: from inks to consumer products to cement. Indeed, different stimuli are already used to tune colloidal gels, from shear flow [53] to magnetic field, if the particles are magnetic. Ultrasound alone is able to tune the properties of certain gels, known as "rheo-acoustic gels" [60], and we have introduced ultrasound-driven bubbles as a new handle. This still leaves us with the unanswered question of how to detect and visualize yielding, which is discussed in the next section.

V. OUTLOOK

This article describes how probing high-frequency rheology with bubble dynamics (Sec. II) bridges a gap in frequency that is important for biomedical applications and industrial processing flows. This is currently an active field with a growing research community. Ongoing developments include design of experiments for optimized bubble-dynamics-based rheometry [61]. Future research should also address the validation of the high-frequency or high-strain-rate measurements with other methods, which is challenging precisely because the bubble-dynamics-based methods fill a gap in frequency that is typically not accessible with other methods.

The article also describes our initial, unsuccessful attempts at removing trapped bubbles from a yield-stress fluid using ultrasound-driven bubble oscillations, which have opened up a different research direction (Sec. III). Indeed, there is currently an active interest both in the bubble dynamics community and in the rheology community to better understand the effect of injection artifacts [52] and the conditions in which bubbles can be removed from yield-stress fluids using external stimuli. Furthermore, advancements in measurement methods may enable the visualization of yielding and the dynamic evolution of the yield surface around bubbles, such as direct mapping of the deformation field [62] or photoelastic imaging [63,64]. Another interesting direction is related to bubble dynamics in complex fluids with other nonlinear behaviors, for instance, shear-thickening fluids which become solid under stress [65].

Finally, the article describes our observation of a flow-induced mechanism triggered by ultrasound-driven bubble dynamics in confinement for locally tuning the microstructure of colloidal gels (Sec. IV). While in this example the global microstructure remains largely homogeneous, this is not always the case for flow-induced microstructures. Future research should probe the limit of a continuum approximation in describing the behavior of complex fluids under the rather extreme deformation conditions of bubble dynamics and cavitation: high frequency and high strain rate.

These future developments will be facilitated by the growing synergy between the communities of bubble dynamics and cavitation, and rheology and soft matter physics, as well as solid mechanics.

ACKNOWLEDGMENTS

I wish to thank all group members, past and present, whose creativity and perseverance have made this work possible. I also wish to thank B. Dollet, J. C. Crocker, M. Jalaal, D. Lohse, P. Marmottant, A. Prosperetti, J. Snoejer, K. J. Stebe, J. Tsamopoulos, and M. Versluis for inspiring discussions on bubble dynamics and complex fluids. The work described in this paper was funded by Starting Grant No. 639221 and Proof of Concept Grant No. 101081830 of the European Research Council.

DATA AVAILABILITY

No data were created or analyzed in this study.

[1] B. Browne and L. Szramek, Rates of magma ascent and storage, in *The Encyclopedia of Volcanoes 2nd ed.*, edited by H. Sigurdsson (Academic Press, 2015), pp. 203–214.

[2] O. Vincent, Negative pressure and cavitation dynamics in plantlike structures, in *Soft Matter in Plants: From Biophysics to Biomimetics*, edited by K. Jensen and Y. Forterre (Royal Society of Chemistry, London, 2022), pp. 119–164.

[3] T. Faez, M. Emmer, K. Kooiman, M. Versluis, A. F. van der Steen, and N. de Jong, 20 years of ultrasound contrast agent modeling, IEEE Trans. Ultrason. Ferroelectr. Freq. Control **60**, 7 (2012).

[4] C. C. Coussios and R. A. Roy, Applications of acoustics and cavitation to noninvasive therapy and drug delivery, Annu. Rev. Fluid Mech. **40**, 395 (2008).

[5] J. Blackmore, S. Shrivastava, J. Sallet, C. R. Butler, and R. O. Cleveland, Ultrasound neuromodulation: A review of results, mechanisms and safety, Ultrasound Med. Biol. **45**, 1509 (2019).
[6] G. Astarita and G. Apuzzo, Motion of gas bubbles in non-Newtonian liquids, AIChE J. **11**, 815 (1965).
[7] G. Pagani, M. J. Green, P. Poulin, and M. Pasquali, Competing mechanisms and scaling laws for carbon nanotube scission by ultrasonication, Proc. Natl. Acad. Sci. USA **109**, 11599 (2012).
[8] B. Dollet, P. Marmottant, and V. Garbin, Bubble dynamics in soft and biological matter, Annu. Rev. Fluid Mech. **51**, 331 (2019).
[9] H. Cochard and S. Delzon, Hydraulic failure and repair are not routine in trees, Ann. For. Sci. **70**, 659 (2013).
[10] J. J. Choi, K. Selert, F. Vlachos, A. Wong, and E. E. Konofagou, Noninvasive and localized neuronal delivery using short ultrasonic pulses and microbubbles, Proc. Natl. Acad. Sci. USA **108**, 16539 (2011).
[11] V. G. Krishnan, L. Fiorucci, A. Sarbu, and W. Drenckhan-Andreatta, Characterizing the foaming process of polymers: Review of experimental methods, Adv. Colloid and Interface Science **344**, 103579 (2025).
[12] A. Lucas, C. Zakri, M. Maugey, M. Pasquali, P. van der Schoot, and P. Poulin, Kinetics of nanotube and microfiber scission under sonication, J. Phys. Chem. C **113**, 20599 (2009).
[13] M. S. Plesset and A. Prosperetti, Bubble dynamics and cavitation, Annu. Rev. Fluid Mech. **9**, 145 (1977).
[14] Rayleigh, On the pressure developed in a liquid during the collapse of a spherical cavity, London, Edinburgh, Dublin Philos. Mag. J. Sci. **34**, 94 (1917).
[15] M. P. Brenner, S. Hilgenfeldt, and D. Lohse, Single-bubble sonoluminescence, Rev. Mod. Phys. **74**, 425 (2002).
[16] A. Prosperetti, Thermal effects and damping mechanisms in the forced radial oscillations of gas bubbles in liquids, J. Acoust. Soc. Am. **61**, 17 (1977).
[17] A. Prosperetti, A generalization of the Rayleigh–Plesset equation of bubble dynamics, Phys. Fluids **25**, 409 (1982).
[18] R. G. Larson, *The Structure and Rheology of Complex Fluids* (Oxford University Press, Oxford, 1999).
[19] C. W. Macosko, *Rheology: Principles, Measurements and Applications* (Wiley-VCH New York, 1994).
[20] H. S. Fogler and J. D. Goddard, Collapse of spherical cavities in viscoelastic fluids, Phys. Fluids **13**, 1135 (1970).
[21] C. C. Church, The effects of an elastic solid surface layer on the radial pulsations of gas bubbles, J. Acoust. Soc. Am. **97**, 1510 (1995).
[22] C. Hua and E. Johnsen, Nonlinear oscillations following the Rayleigh collapse of a gas bubble in a linear viscoelastic (tissue-like) medium, Phys. Fluids **25**, 083101 (2013).
[23] J. S. Allen and R. A. Roy, Dynamics of gas bubbles in viscoelastic fluids. II. Nonlinear viscoelasticity, J. Acoust. Soc. Am. **108**, 1640 (2000).
[24] J. Jiménez-Fernández and A. Crespo, Bubble oscillation and inertial cavitation in viscoelastic fluids, Ultrasonics **43**, 643 (2005).
[25] J. Naude and F. Méndez, Periodic and chaotic acoustic oscillations of a bubble gas immersed in an upper convective maxwell fluid, J. Non-Newtonian Fluid Mech. **155**, 30 (2008).
[26] M. T. Warnez and E. Johnsen, Numerical modeling of bubble dynamics in viscoelastic media with relaxation, Phys. Fluids **27**, 063103 (2015).
[27] R. Gaudron, M. T. Warnez, and E. Johnsen, Bubble dynamics in a viscoelastic medium with nonlinear elasticity, J. Fluid Mech. **766**, 54 (2015).
[28] A. T. Oratis, K. Dijs, G. Lajoinie, M. Versluis, and J. H. Snoeijer, A unifying Rayleigh-Plesset-type equation for bubbles in viscoelastic media, J. Acoust. Soc. Am. **155**, 1593 (2024).
[29] B. Saint-Michel and V. Garbin, Bubble dynamics for broadband microrheology of complex fluids, Curr. Opin. Colloid Interface Sci. **50**, 101392 (2020).
[30] P. S. Epstein and M. S. Plesset, On the stability of gas bubbles in liquid-gas solutions, J. Chem. Phys. **18**, 1505 (1950).
[31] W. Kloek, T. Van Vliet, and M. Meinders, Effect of bulk and interfacial rheological properties on bubble dissolution, J. Colloid Interface Sci. **237**, 158 (2001).
[32] J. B. Estrada, C. Barajas, D. L. Henann, E. Johnsen, and C. Franck, High strain-rate soft material characterization via inertial cavitation, J. Mech. Phys. Solids **112**, 291 (2018).

[33] A. Jamburidze, M. De Corato, A. Huerre, A. Pommella, and V. Garbin, High-frequency linear rheology of hydrogels probed by ultrasound-driven microbubble dynamics, Soft Matter **13**, 3946 (2017).
[34] K. Ando and E. Shirota, Quasistatic growth of bubbles in a gelatin gel under dissolved-gas supersaturation, Phys. Fluids **31**, 111701 (2019).
[35] L. Mancia, J. Yang, J.-S. Spratt, J. R. Sukovich, Z. Xu, T. Colonius, C. Franck, and E. Johnsen, Acoustic cavitation rheometry, Soft Matter **17**, 2931 (2021).
[36] J.-S. Spratt, M. Rodriguez, K. Schmidmayer, S. H. Bryngelson, J. Yang, C. Franck, and T. Colonius, Characterizing viscoelastic materials via ensemble-based data assimilation of bubble collapse observations, J. Mech. Phys. Solids **152**, 104455 (2021).
[37] Z. Zhu, S. Remillard, B. A. Abeid, D. Frolkin, S. H. Bryngelson, J. Yang, M. Rodriguez, and J. B. Estrada, Parsimonious inertial cavitation rheometry via bubble collapse time, Soft Matter **21**, 6717 (2025).
[38] S. M. van der Meer, B. Dollet, M. M. Voormolen, C. T. Chin, A. Bouakaz, N. de Jong, M. Versluis, and D. Lohse, Microbubble spectroscopy of ultrasound contrast agents, J. Acoust. Soc. Am. **121**, 648 (2007).
[39] E. Hersey Jr., M. Rodriguez, and E. Johnsen, Dynamics of an oscillating microbubble in a blood-like carreau fluid, J. Acoust. Soc. Am. **153**, 1836 (2023).
[40] A. van der Bos, M.-J. van der Meulen, T. Driessen, M. van den Berg, H. Reinten, H. Wijshoff, M. Versluis, and D. Lohse, Velocity profile inside piezoacoustic inkjet droplets in flight: Comparison between experiment and numerical simulation, Phys. Rev. Appl. **1**, 014004 (2014).
[41] N. J. Balmforth, I. A. Frigaard, and G. Ovarlez, Yielding to stress: Recent developments in viscoplastic fluid mechanics, Annu. Rev. Fluid Mech. **46**, 121 (2014).
[42] J. Tsamopoulos, Y. Dimakopoulos, N. Chatzidai, G. Karapetsas, and M. Pavlidis, Steady bubble rise and deformation in newtonian and viscoplastic fluids and conditions for bubble entrapment, J. Fluid Mech. **601**, 123 (2008).
[43] M. Zare, M. Daneshi, and I. Frigaard, Effects of nonuniform rheology on the motion of bubbles in a yield-stress fluid, J. Fluid Mech. **919**, A25 (2021).
[44] E. Chaparian and I. A. Frigaard, Clouds of bubbles in a viscoplastic fluid, J. Fluid Mech. **927**, R3 (2021).
[45] M. Daneshi and I. A. Frigaard, Growth and static stability of bubble clouds in yield stress fluids, J. Non-Newtonian Fluid Mech. **327**, 105217 (2024).
[46] M. De Corato, B. Saint-Michel, G. Makrigiorgos, Y. Dimakopoulos, J. Tsamopoulos, and V. Garbin, Oscillations of small bubbles and medium yielding in elastoviscoplastic fluids, Phys. Rev. Fluids **4**, 073301 (2019).
[47] B. Saint-Michel and V. Garbin, Acoustic bubble dynamics in a yield-stress fluid, Soft Matter **16**, 10405 (2020).
[48] G. Karapetsas, D. Photeinos, Y. Dimakopoulos, and J. Tsamopoulos, Dynamics and motion of a gas bubble in a viscoplastic medium under acoustic excitation, J. Fluid Mech. **865**, 381 (2019).
[49] P. Saramito, A new elastoviscoplastic model based on the Herschel–Bulkley viscoplastic model, J. Non-Newtonian Fluid Mech. **158**, 154 (2009).
[50] L. Martinie, H. Buggisch, and N. Willenbacher, Apparent elongational yield stress of soft matter, J. Rheol. **57**, 627 (2013).
[51] K. Murakami, R. Gaudron, and E. Johnsen, Shape stability of a gas bubble in a soft solid, Ultrason. Sonochem. **67**, 105170 (2020).
[52] A. Pourzahedi, M. Zare, and I. Frigaard, Eliminating injection and memory effects in bubble rise experiments within yield stress fluids, J. Non-Newtonian Fluid Mech. **292**, 104531 (2021).
[53] N. Koumakis, E. Moghimi, R. Besseling, W. C. Poon, J. F. Brady, and G. Petekidis, Tuning colloidal gels by shear, Soft Matter **11**, 4640 (2015).
[54] B. Saint-Michel, G. Petekidis, and V. Garbin, Tuning local microstructure of colloidal gels by ultrasound-activated deformable inclusions, Soft Matter **18**, 2092 (2022).
[55] P. Marmottant and S. Hilgenfeldt, Controlled vesicle deformation and lysis by single oscillating bubbles, Nature (London) **423**, 153 (2003).
[56] P. Marmottant, M. Versluis, N. De Jong, S. Hilgenfeldt, and D. Lohse, High-speed imaging of an ultrasound-driven bubble in contact with a wall: "Narcissus" effect and resolved acoustic streaming, Exp. Fluids **41**, 147 (2006).

[57] R. Bolaños-Jiménez, M. Rossi, D. F. Rivas, C. J. Kähler, and A. Marin, Streaming flow by oscillating bubbles: Quantitative diagnostics via particle tracking velocimetry, J. Fluid Mech. **820**, 529 (2017).

[58] F. Mekki-Berrada, T. Combriat, P. Thibault, and P. Marmottant, Interactions enhance the acoustic streaming around flattened microfluidic bubbles, J. Fluid Mech. **797**, 851 (2016).

[59] K. W. Torre and J. de Graaf, Structuring colloidal gels via micro-bubble oscillations, Soft Matter **19**, 2771 (2023).

[60] T. Gibaud, N. Dagès, P. Lidon, G. Jung, L. C. Ahouré, M. Sztucki, A. Poulesquen, N. Hengl, F. Pignon, and S. Manneville, Rheoacoustic gels: Tuning mechanical and flow properties of colloidal gels with ultrasonic vibrations, Phys. Rev. X **10**, 011028 (2020).

[61] T. Chu, J. B. Estrada, and S. H. Bryngelson, Bayesian optimal design accelerates discovery of soft material properties from bubble dynamics, Comput. Mech. **76**, 431 (2025).

[62] A. McGhee III, J. Yang, E. Bremer, Z. Xu, H. Cramer III, J. Estrada, and D. Henann, High-speed, full-field deformation measurements near inertial microcavitation bubbles inside viscoelastic hydrogels, Expt. Mech. **63**, 63 (2023).

[63] J. Rapet, Y. Tagawa, and C.-D. Ohl, Shear-wave generation from cavitation in soft solids, Appl. Phys. Lett. **114**, 123702 (2019).

[64] Y. Yokoyama, B. R. Mitchell, A. Nassiri, B. L. Kinsey, Y. P. Korkolis, and Y. Tagawa, Integrated photoelasticity in a soft material: Phase retardation, azimuthal angle, and stress-optic coefficient, Optics Lasers Eng. **161**, 107335 (2023).

[65] G. T. Bokman, O. Supponen, and S. A. Mäkiharju, Cavitation bubble dynamics in a shear-thickening fluid, Phys. Rev. Fluids **7**, 023302 (2022).